



Published in final edited form as:

Circulation. 2009 August 4; 120(5): 408–416. doi:10.1161/CIRCULATIONAHA.109.865154.

Repair of acute myocardial infarction with iPS induced by human stemness factors

Timothy J. Nelson, MD, PhD, Almudena Martinez-Fernandez, PharmD, Satsuki Yamada, MD, PhD, Carmen Perez-Terzic, MD, PhD, Yasuhiro Ikeda, DVM, PhD, and Andre Terzic, MD, PhD
Division of Cardiovascular Diseases, Departments of Medicine, Molecular Pharmacology and Experimental Therapeutics, and Medical Genetics, Mayo Clinic, Rochester, MN (T.J.N., A.M.F., S.Y., C.P.T., A.T.); Department of Physical Medicine and Rehabilitation, Mayo Clinic, Rochester, MN (C.P.T.); Department of Molecular Medicine (Y.I.), Mayo Clinic, Rochester, MN

Abstract

Background—Nuclear reprogramming provides an emerging strategy to produce embryo-independent pluripotent stem cells from somatic tissue. Induced pluripotent stem cells (iPS) demonstrate aptitude for *de novo* cardiac differentiation, yet their potential for heart disease therapy has not been tested.

Methods and Results—Here, fibroblasts transduced with human stemness factors OCT3/4, SOX2, KLF4, and c-MYC converted into an embryonic stem cell-like phenotype and demonstrated the ability to spontaneously assimilate into preimplantation host morula *via* diploid aggregation, unique to *bona fide* pluripotent cells. *In utero*, iPS-derived chimera executed differentiation programs to construct normal heart parenchyma patterning. Within infarcted hearts in the adult, intramyocardial delivery of iPS yielded progeny that properly engrafted without disrupting cytoarchitecture in immunocompetent recipients. In contrast to parental non-reparative fibroblasts, iPS treatment restored post-ischemic contractile performance, ventricular wall thickness and electrical stability while achieving *in situ* regeneration of cardiac, smooth muscle and endothelial tissue.

Conclusion—Fibroblasts reprogrammed by human stemness factors thus acquire the potential to repair acute myocardial infarction, establishing iPS in the treatment of heart disease.

Keywords

transplantation; induced pluripotent stem cells; regenerative medicine

Correspondence to Andre Terzic, MD, PhD, Mayo Clinic, 200 First Street SW, Rochester, MN 55905; Fax: (507) 266-9936; Phone: (507) 284-2747; E-mail: terzic.andre@mayo.edu.

Disclosures: None

Triggered nuclear reprogramming through ectopic transgene expression of stemness factors offers a revolutionary strategy for embryo-independent derivation of pluripotent stem cells from an ordinary adult source. Induced pluripotent stem cell (iPS) technology invalidates chronological age, reversing cell fate to reset an atavistic embryonic-like potential of somatic tissue. In this way, iPS have attained functions previously demonstrated only by natural embryonic stem cells to independently produce all tissues types and develop the complete organism within an embryonic environment. Here, fibroblasts redirected by a foursome of human stemness factors, OCT3/4, SOX2, KLF4 and c-MYC, acquired *bona fide* pluripotent features ensuring *de novo* tissue replacement in embryonic and adult host environments. Head-to-head comparison between parental fibroblasts and reprogrammed progeny established the therapeutic value for cardiac tissue regeneration in a setting of ischemic heart disease. Specifically, transplantation of iPS in the acutely infarcted myocardium yielded structural and functional repair to secure performance recovery as qualified clones contributed to *in vivo* tissue reconstruction with “on-demand” cardiovascularogenesis. Although the full clinical impact of iPS-based technology will be revealed when safeguards are fully validated, the proof-of-principle study here establishes the practical application of bioengineered stem cells to respond to the ischemic myocardium and heal the damaged areas with iPS-derived integrated functional tissues. Therefore, converting self-derived fibroblasts, main contributors to post-ischemic scar, into reparative progenitors can now be considered as a goal of regenerative medicine to individualize treatment algorithms for multi-lineage cardiovascular repair.

Regenerative medicine offers the potential of curative therapy to repair damaged tissues.^{1,2} Pluripotent stem cells derived from the inner cell mass of early stage embryos have provided a prototype for multi-lineage repair. Ethical considerations along with practical limitations have however precluded adoption of embryonic stem cell platforms, driving advances in nuclear reprogramming to establish viable alternatives.³ In this regard, induced pluripotent stem cell (iPS) technology provides an emerging innovation that promises the unlimited potential of embryonic stem cells while circumventing the need for embryonic sources.⁴

Nuclear reprogramming designed to convert somatic tissues into stem cells capable of germline transmission has been recently achieved with ectopic expression of various pluripotent gene combinations.⁵⁻⁸ Delivery of stemness-related gene sets, exemplified by the Oct-3/4, Sox2, Klf4 and c-Myc quartet,⁵ reprograms adult somatic cells by promoting re-acquisition of evolutionarily conserved embryonic gene networks.⁹ By reinstating pluripotency, iPS reset the biological age of a cell reflected in the re-lengthening of telomeres.¹⁰ The potential for reversing adult cell fates has been systematically exploited, producing iPS from diverse tissue origins across phylogenetic barriers.^{11,12}

Although induced pluripotency reliably generates an embryonic-like ground state from healthy and diseased sources,^{13,14} the therapeutic value of reprogramming remains largely unknown. To date, only three disease models have been treated with iPS-derived strategies.¹⁵⁻¹⁷ Interventions in sickle cell anemia, Parkinson's disease, and hemophilia A have been limited to lineages pre-specified *in vitro*.¹⁵⁻¹⁷ Despite recapitulating the cardiomyogenic phenotype from both murine and human somatic fibroblasts,¹⁸⁻²¹ multi-lineage repair of heart tissue with iPS-based intervention has yet to be documented.

We here demonstrate for the first time the efficacy of iPS to treat acute myocardial infarction. Murine fibroblasts were transduced with human stemness-related factors through an efficient vector system to generate valid iPS clones with inherent cardiogenic potential. Head-to-head comparison between parental fibroblasts and reprogrammed progeny established the acquired propensity for cardiac tissue regeneration in a setting of ischemic heart disease. iPS progeny engrafted in the context of immunocompetent allogeneic transplantation, and rescued post-ischemic myocardial structure and function. This proof-of-principle study pioneers fibroblast-derived iPS in cardiac repair.

Methods

Protocols were approved by the Institutional Animal Care and Use Committee.

Transduction

pSIN-CSGWdINotI-derived transfer vectors were generated with human OCT3/4, SOX2, KLF4 and c-MYC cDNAs (Open Biosystems).²² The packaging plasmid, pCMVR8.91, was engineered with H87Q mutation in the HIV-1 capsid region for increased transduction efficiency of purified infectious supernatants.²² Mouse embryonic fibroblasts, obtained from embryos at 14.5 days post-coitum (dpc), were expanded in maintenance medium containing Dulbecco's modified Eagle's medium (Invitrogen) supplemented with 10% fetal calf serum (FCS), 1% L-glutamine (Invitrogen) and 1% penicillin/streptomycin, and plated at 10⁵/24-wells prior to transduction for 12 h with infectious supernatants. Transduced fibroblasts were replated at confluence, and iPS isolated in 2 weeks for clonal expansion. Cells were labeled with HIV vectors carrying LacZ (pLenti6/Ubc/V5-GW/LacZ, Invitrogen) or luciferase (pSIN-Luc).²³

Pluripotent induction

R1-derived embryonic stem cells and iPS were expanded in embryonic stem cell media. Cells were fixed with 3% paraformaldehyde, permeabilized and stained with anti-SSEA-1 antibody (MAB4301; dilution 1:50; Chemicon) along with secondary goat anti-mouse Alexa Fluor 568 (1:250; Invitrogen). Nuclei were labeled with 4,6'-diamidino-2-phenylindole (DAPI; Invitrogen). For ultrastructural evaluation, cells were examined on Hitachi 4700 field emission scanning or JEOL 1200 EXII transmission electron microscopes.²⁴ Growth and differentiation potential were determined upon subcutaneous injection in anesthetized (2-3% isoflurane) athymic nude mice. Cryopreserved tissue was processed for hematoxylin/eosin procedures.^{25,26}

Differentiation

iPS were differentiated into embryoid bodies using the hanging-drop method.²⁷ Expression of pre-cardiac mesoderm and cardiac differentiation markers was detected by RT-PCR. Total RNA was extracted with a combination of gDNA Eliminator and RNeasy columns (Qiagen). cDNA was prepared from RNA samples using Superscript III First Strand Synthesis System (Invitrogen). Mouse *Gapdh* (4352932E; Applied Biosystems) was used as control. Analyzed genes included *Gata4* (Mm00484689_m1), *Myocd* (Mm00455051_m1), and *Mef2c* (Mm01340839_m1; Applied Biosystems).

Diploid aggregation

Contribution to embryonic development was assessed through diploid aggregation.²⁸ Host embryos from CD-1 superovulated females were collected at 2.5 dpc. Fibroblasts or iPS were partially digested using trypsin 0.25%-EDTA (Invitrogen), and 8-15 cell clumps were placed with paired embryos denuded of zona pellucida. The aggregation complex was incubated for 24 h (in 5% CO₂/5% O₂/90% N₂) until blastocyst cavitation.²⁸ Chimeric embryos were transplanted into anesthetized (2-3% isoflurane) pseudopregnant surrogate CD-1 mothers, harvested at 9.5 dpc, and analyzed for distribution of LacZ-labeled progenitors.²⁸

iPS therapy

Male, 8-12 weeks old C57BL/6 or athymic nude mice were anesthetized (1.5-2% isoflurane), intubated (Mini Vent 845, Hugo Sacks Elektronik), and left coronary artery ligated with a 9-0 suture under direct visualization following minimally invasive thoracotomy. Myocardial ischemia was confirmed by electrocardiography, echocardiography, and color change of left ventricular wall. Fibroblasts or iPS (200,000/10 μ l of differentiation medium) were transplanted with four injections of 2.5 μ l within 30 min after ligation. Cryosections (7 μ m-thickness) were processed for hematoxylin/eosin, Masson's trichrome, luciferase and β -gal staining.^{25,26} Sections were labeled with luciferase (1:5000, Sigma) or β -galactosidase antibody (1:5000, Abcam) coupled with Alexa-568 secondary antibody (1:1000, Invitrogen) and co-localized with α -actinin (1:200, Sigma), smooth muscle actin (1:200, Abcam), CD31 (1:200, Abcam), or SSEA-1 (1:50, Chemicon) antibodies all paired with Alexa-488 antibody (1:1000, Invitrogen).

Live cell imaging and heart performance

Luciferase-transfected fibroblasts or iPS were cultured for multiple passages including a freeze/thaw cycle prior to expansion and transplantation. Cells were tracked with the IVIS 200 Bioluminescence Imaging System (Xenogen) following intra-peritoneal injection of 150 mg/kg D-luciferin (Xenogen), and signals analyzed with the Living Image Software (Xenogen). Ventricular performance was quantified by echocardiography (RMV-707B scanhead, Vevo770, Visual Sonics). Ejection fraction (%) was calculated as $[(LVVd - LVVs)/LVVd] \times 100$, where LVVd is left ventricular end-diastolic volume (μ L) and LVVs, left ventricular end-

systolic volume (μL). Left ventricular fractional shortening (% FS) was calculated as $[(\text{LVDd} - \text{LVDs})/\text{LVDd}] \times 100$, where LVDd is left ventricular end-diastolic dimension (mm) and LVDs, left ventricular end-systolic dimension (mm).²⁵ Electrical activity was monitored by electrocardiography (MP150, Biopac). Data was collected and analyzed by blinded investigators.

Statistical analysis

Results are presented as mean \pm SEM. Median is additionally reported when grouped data were compared with nonparametric Mann-Whitney *U* test. Comparison between groups over time was performed by two-way repeated-measures ANOVA. Kaplan-Meier analysis was applied with log-rank testing. $p < 0.05$ was predetermined as significant, and all values > 0.001 were reported.

Results

Nuclear reprogramming resets primitive morphology and unlocks functional pluripotency

Transduced with human stemness factors, OCT3/4, KLF4, SOX2 and c-MYC, reprogrammed fibroblasts were isolated according to compact clusters of embryonic stem cell-like morphology distinct from monomorphic, single-cell layers of parental fibroblasts (Figure 1A). Reprogrammed cells displayed distinct sub-cellular architecture, reorganized from original fibroblasts to recapitulate salient features of undifferentiated embryonic stem cells with high nucleocytoplasmic ratio, predominance of nuclear euchromatin and scant density of cytosolic organelles (Figure 1B). Reprogramming induced expression of the early embryonic SSEA-1 antigen, an initial marker of stemness absent in parental fibroblasts (Figure 1C). To determine functional pluripotency, the inherent capacity for embryonic integration was probed by diploid aggregation using a pair of denuded host embryos (Figure 1D, upper). While morula-derived blastomeres incorporated into an embryonic structure after 24 h in micro-wells, fibroblasts aborted engraftment and failed to contribute to *ex utero* blastocyst development (Figure 1D, lower left). In contrast, reprogrammed fibroblasts demonstrated spontaneous integration and contributed to pre-implantation blastocyst formation (Figure 1D, lower right). Non-coerced assimilation into early stage embryos thereby established *bona fide* iPS clones, providing a high-stringency quality control measure for functional pluripotency.

Chimeric embryos authenticate iPS-derived patterning of normal cardiogenesis

As iPS differentiated within 5-day-old embryoid bodies (Figure 2A), up-regulation of pre-cardiac markers *Mesp1*, *Tbx5*, *Cxcr4*, and *Flk-1* indicated engagement beyond the original fibroblast lineage^{29,30} (not illustrated). Within 12 days, increased expression of canonical cardiac transcription factors, *Mef2c* ($p=0.049$; $n=3$), *Gata4* ($p=0.049$; $n=3$) and *Myocardin* ($p=0.049$; $n=3$), indicated the capacity for cardiac tissue maturation (Figure 2B). Beyond redirection of somatic cell fate *in vitro*, chimeric embryos were utilized to examine the ability of iPS clones to ensure tissue formation during embryonic development *in utero*. Pre-implantation blastocysts containing lacZ-labeled iPS progenitors were transferred into surrogate uterus, and tracked at early stages of organogenesis. iPS labeled with a constitutively active reporter construct mimicked the stochastic distribution of embryonic stem cells throughout the developing embryo at 9.5 dpc (Figure 2C). Labeled iPS progeny demonstrated robust contribution to the heart field, including cardiac inflow and outflow tracts as well as left and right ventricles of the embryonic heart parenchyma (Figure 2D and 2E). Thereby, qualified iPS clones demonstrated *de novo* organogenesis and patterning of cardiogenic tissue within a developing embryo.

iPS engraft into infarcted immunocompetent adult hearts

In contrast to fibroblasts unable to proliferate even after prolonged incubation, subcutaneous injection of iPS clones within an immunodeficient adult environment demonstrated aggressive growth (Figure 3A). Transplanted cells, initially labeled with retroviral reporter constructs and expanded through multiple passages (>5) *in vitro*, were tracked with *in vivo* imaging using emitted bioluminescence from iPS-derived progeny. Upon permanent occlusion of epicardial coronary vasculature and microsurgical transfer into the ischemic myocardium, iPS remained within injected hearts and produced gradual tumor outgrowth between 2-4 weeks (Figure 3B). Echocardiography confirmed a significant tumor burden, which compromised hemodynamics 4-weeks post-transplant (Figure 3C). Autopsy in immunodeficient recipients (n=6) verified consistent teratoma formation with extension beyond the myocardial wall and tumor infiltration within the post-injured myocardium (Figure 3C). In contrast to tumorigenesis that compromised the safety within immunodeficient environments, subcutaneous transplantation of iPS into immunocompetent hosts demonstrated a persistent absence of tumor growth in all animals (n=6) even at 8 weeks of follow-up (Figure 3D). Furthermore, intramyocardial transplantation of 200,000 iPS/heart, a dose selected based on tumor-free outcome with embryonic stem cell intervention,^{26,27} produced stable engraftment without detectable tumor formation (n=6; Figure 3E). According to bioluminescence emitted from labeled progeny, differentiated iPS within ischemic immunocompetent hearts were detectable by 2 weeks post-transplantation without metastatic dissemination after 4 weeks of engraftment (n=6; Figure 3E). In fact, immunostaining of hearts at 4 weeks demonstrated rare iPS progeny positive for SSEA-1 expression within the post-ischemic myocardium (Figure 3F). Immunocompetent recipients thus ensured controlled iPS engraftment (Figure 3G) with tissue integration that did not perturb electrical homeostasis (n=6; Figure 3H). In this way, the immunocompetent adult host provided a permissive environment for differentiation, offering the opportunity to test the therapeutic potential of iPS clones.

iPS therapy restores myocardial performance lost by ischemic injury

Within immunocompetent hosts, recovery of post-ischemic cardiac performance was compared in randomized cohorts transplanted with parental fibroblasts *versus* derived iPS. Monitored by echocardiography, irreversible occlusion of the epicardial coronary blood flow consistently impaired anterior wall motion, depressed global cardiac function, and halved ejection fraction (EF) from $82\pm 3\%$ before infarction (n=8) to $38\pm 3\%$ within 1-day post-infarction (n=12; Figure 4A). While blinded transplantation with parental fibroblasts demonstrated persistent functional decline with EF dropping to $37\pm 4\%$ at 4 weeks (n=6), iPS intervention improved cardiac contractility to achieve an EF of $56\pm 2\%$ within the first 2-weeks of therapy and $50\pm 5\%$ by 4 weeks (n=6; $p=0.002$ iPS *versus* fibroblasts, Figure 4A). Functional benefit in response to iPS was verified by the improved fractional shortening, from $20\pm 1\%$ (median 18%, n=6) at 1-day post-infarction to $31\pm 3\%$ (median 29%, n=6) after 4-weeks, in contrast to a lack of recovery in fibroblast-treated hearts (n=6, $p=0.01$; Figure 4B). Moreover, the regional septal wall thickness in systole was significantly rebuilt with iPS (1.31 ± 0.11 mm, median 1.20 mm, n=5), but not with fibroblast (0.88 ± 0.06 mm, median 0.90 mm, n=6) treatment ($p=0.006$; Figure 4C). Impaired cardiac contractility in the injured anterior wall resulted in akinetic regions with paradoxical motion in systole indicative of aneurysms in fibroblast-treated hearts, in contrast to coordinated concentric contractions in response to iPS treatment visualized by long-axis and short-axis imaging (Figure 4D and 4E). Thus, compared to non-reparative parental fibroblasts, iPS intervention improved functional performance following acute myocardial infarction.

iPS therapy halts progression of pathologic remodeling in infarcted hearts

Beyond functional deterioration, maladaptive remodeling with detrimental structural changes prognosticates poor outcome following ischemic injury. Here, iPS-based intervention attenuated global left ventricular diastolic diameter (LVDD). Pre-infarction LVDD measured 3.2 ± 0.1 mm (median 3.1 mm), but increased post-infarction to 4.9 ± 0.1 mm (median 4.9 mm) by 4-weeks of fibroblast treatment (n=6) a value significantly higher ($p=0.007$) than 4.2 ± 0.2 mm (median 4.2 mm) with iPS treatment (n=6; Figure 5A). Furthermore, echocardiography demonstrated regional structural deficits with deleterious wall thinning and chamber dilation in fibroblast-treated hearts (n=6), rescued by iPS intervention (n=6; Figure 5B). Pathologic structural remodeling leads to electrophysiological consequences with prolongation of the QT interval, which increases risk of arrhythmia. Infarction increased QT interval from 28.9 ± 1.4 ms (median 28.1 ms) to 55.9 ± 1.3 ms (median 55.8 ms) in fibroblast-treated hearts (n=6), which was abrogated to 40.8 ± 1.5 ms (median 40.3 ms, n=6) with iPS treatment ($p=0.004$, Figure 5C). These real-time surrogates for tissue remodeling were confirmed on autopsy on inspection of gross specimen that demonstrated reduced heart size, lack of aneurysmal formation, and absence of severe wall thinning in iPS compared to fibroblast-treated hearts (Figure 5D). Collectively, the favorable remodeling at global, regional and electrical level demonstrates overall benefit of iPS therapy in the setting of myocardial infarction.

Multi-lineage cardiac tissue regeneration following iPS therapy

Histological analysis demarcated de-muscularization and extensive scarring within left ventricles distal to coronary ligation in hearts treated with fibroblasts 4 weeks following transplantation (Figure 6A). In contrast, iPS treatment halted structural deterioration of infarcted tissue with anti-fibrotic benefit and remuscularization within the left ventricular free wall (Figure 6A). Surgical dissection and postmortem histopathological analysis verified absence of tumor infiltration or dysregulated cell expansion following iPS transplantation in the myocardium itself, as well as in the liver, lung and spleen - organs with high metastatic risk (n>10 staggered sections throughout respective organs; Figure 6B). In post-ischemic myocardium, immunohistochemistry confirmed engraftment of iPS-derived progeny that expressed transgene markers luciferase (not illustrated) or β -galactosidase (Figure 6C-E). Co-localization of transgene expression with cardiac α -actinin was consistent within the damaged territory as documented by microscopy of serial transverse sections (n>10 at 10-20 μ m intervals) immediately adjacent to the site of coronary ligation (Figure 6C). Smooth muscle α -actin (Figure 6D) and endothelial CD31 (Figure 6E) were also detectable, albeit at lower frequency, consistent with multi-lineage cardiovascular differentiation of iPS. Thus, in contrast to ineffective parental fibroblasts, targeted delivery of iPS generated *de novo* cardiovascular tissue in post-ischemic adult myocardium.

Discussion

Nuclear reprogramming with iPS technology offers embryo-independent pluripotent progenitors. While enabling patient-specific regenerative platforms,³¹ prior to this study iPS have been limited to three non-cardiac disease conditions, namely sickle cell anemia, Parkinson's disease and hemophilia A.¹⁵⁻¹⁷ The present study expands the therapeutic indications of iPS by providing first evidence for repair in the context of heart disease.

The ability to reprogram somatic tissue and reactivate atavistic functions of pluripotency has forged a new strategy for regenerative biology.³¹⁻³⁴ Somatic cell nuclear transfer provided the initial empiric evidence for epigenetic conversion of non-stem cells to acquire pluripotency.³⁵ More recently, nuclear reprogramming has been induced with the minimal requirement of ectopic gene expression of stemness factors.^{36,37} High-stringency testing for *bona fide* pluripotency has been restricted to low-throughput procedures, such as germline transmission

and tetraploid aggregation.^{6,7} Non-coerced diploid aggregation, presented here, offers a rapid yet reliable surrogate marker for functional pluripotency with definitive readout feasible within 24 h. Acquired pluripotency from somatic fibroblasts was herein verified by the inability of parental, non-reprogrammed counterparts to contribute to blastocyst development. As iPS technology continues to advance,³⁶⁻³⁸ diploid aggregation techniques offers thereby a high-throughput functional assay to screen for the pluripotent state of a clonal progenitor population.

Stem cell-based repair integrates multifactorial mechanisms with cardiac regeneration predicated on the ability of diseased myocardium to be replenished with healthy multi-lineage tissue.³⁹⁻⁴⁵ Rejuvenation can be achieved from endogenous stem cell pools that respond to injury, albeit at levels typically insufficient to compensate for severe cardiac damage.³⁹ Exogenous stem cell types have been employed to augment therapeutic healing through paracrine mediated mechanisms⁴⁰ and/or cell-autonomous contribution to tissue reconstruction.^{41,42} In this way, embryonic stem cells have reproduced the complete cellular repertoire within ischemic heart,⁴³⁻⁴⁵ and have demonstrated the ability to augment the physical force of cardiac contraction upon transplantation.⁴⁵ The present study introduces iPS therapy into a diseased myocardium as an alternative to produce cardiogenic tissue independently of an embryonic source. The iPS platform for cell-based regeneration relies on the acquired ground state of pluripotency to enable somatic tissue-derived cardiopoiesis, here validated by *in vitro* differentiation with canonical cardiac transcription factor expression and *in utero* organogenesis with heart parenchyma patterning. Live-cell imaging documented *in situ* reconstruction of damaged tissues and engraftment of iPS-derived progeny within the heart, as transplanted cells were extensively processed to avoid carry-over of lentiviral particles that could cross-contaminate native tissue and confound analysis of *in vivo* cell tracking.^{46, 47} Intramyocardial transplantation of parental fibroblasts within acutely infarcted tissue was unproductive, despite previous indications that a multitude of cell types may improve cardiac function.⁴⁸ In contrast, iPS responded to cardiac injury with controlled integration and chimeric tissue formation within allogeneic host. Cell integration translated into performance recovery as qualified iPS clones contributed to tissue reconstruction with synchronized cardiovascularogenesis, composed predominantly of cardiac lineage with accompanying smooth muscle and endothelium. Although multiple mechanisms likely contribute to the benefit associated with iPS-based therapy, converting fibroblasts, main contributors to post-ischemic scar, into reparative progenitors can thus now be considered as a goal to engage and promote *de novo* tissue repair.

The heterogeneity inherent to the epigenetics and gene expression profiles within pluripotent cells raises however concern for pleiotropic outcomes.^{2,21,49} Both embryonic stem cells and iPS harbor the potential risk of producing teratoma. The propensity for uncontrolled growth of embryonic stem cells is nevertheless modulated by the immunity of non-native environment, as here demonstrated for iPS within adult immunocompetent hosts. A properly matched milieu, such as that of the developing embryo, furthermore ensures precise differentiation and *in utero* growth.²⁸ Diploid aggregation, utilizing the chimeric environment, revealed the reliability of iPS clones to orchestrate tissue patterns without triggering tumorigenic outgrowth, in line with tumor-free organogenesis of iPS offspring.^{3,6,7} Fully differentiated cell types, such as native fibroblasts used here, are in contrast unable to contribute to primordial embryo or heart repair. Exemplified by the inability to integrate into the electrical syncytium of failing myocardium, transplantation of non-stem cell progeny has been plagued by the rigidity associated with advanced fate.^{48,50} Accordingly, the risk-benefit of iPS-based interventions will critically depend on the state of lineage differentiation and the interface with host milieu.

In conclusion, this study expands the therapeutic potential of iPS treatment from non-cardiac to cardiac disease. Created by ectopic expression of four human stemness related factors, iPS demonstrated acquired cardiogenicity, and ensured functional and structural repair of infarcted

myocardium. While individual iPS clones are likely to exhibit a spectrum of reparative potential, advances in nuclear reprogramming provide the tools to customize the reversibility of cell fate for “on-demand” cardiovascular regenerative medicine.

Acknowledgments

We thank Jonathan Nesbitt for surgical expertise and Lois Rowe for histological analysis.

Funding Sources: Supported by National Institutes of Health (R01HL083439, T32HL007111, R01HL085208, R56AI074363), American Heart Association, American Society for Clinical Pharmacology and Therapeutics, National Hemophilia Foundation, La Caixa Foundation Graduate Program, Marriott Individualized Medicine Program, Marriott Heart Disease Research Program, and Mayo Foundation.

References

1. Daley GQ, Scadden DT. Prospects for stem cell-based therapy. *Cell* 2008;132:544–548. [PubMed: 18295571]
2. Segers V, Lee RT. Stem-cell therapy for cardiac disease. *Nature* 2008;451:937–942. [PubMed: 18288183]
3. Yamanaka S. Strategies and new developments in the generation of patient-specific pluripotent stem cells. *Cell Stem Cell* 2007;1:39–49. [PubMed: 18371333]
4. Nishikawa S, Goldstein RA, Nierras CR. The promise of human induced pluripotent stem cells for research and therapy. *Nat Rev Mol Cell Biol* 2008;9:725–729. [PubMed: 18698329]
5. Takahashi K, Okita K, Nakagawa M, Yamanaka S. Induction of pluripotent stem cells from mouse embryonic and adult fibroblast cultures by defined factors. *Cell* 2006;126:663–676. [PubMed: 16904174]
6. Okita K, Ichisaka T, Yamanaka S. Generation of germline-competent induced pluripotent stem cells. *Nature* 2007;448:313–317. [PubMed: 17554338]
7. Wernig M, Meissner A, Foreman R, Brambrink T, Ku M, Hochedlinger K, Bernstein BE, Jaenisch R. In vitro reprogramming of fibroblasts into a pluripotent ES-cell-like state. *Nature* 2007;448:318–324. [PubMed: 17554336]
8. Yu J, Vodyanik MA, Smuga-Otto K, Antosiewicz-Bourget J, Frane JL, Tian S, Nie J, Jonsdottir GA, Ruotti V, Stewart R, Slukvin II, Thomson JA. Induced pluripotent stem cell lines derived from human somatic cells. *Science* 2007;318:1917–1920. [PubMed: 18029452]
9. Silva J, Barrandon O, Nichols J, Kawaguchi J, Theunissen TW, Smith A. Promotion of reprogramming to ground state pluripotency by signal inhibition. *PLoS Biol* 2008;6:e253. [PubMed: 18942890]
10. Marion RM, Strati K, Li H, Tejera A, Schoeftner S, Ortega S, Serrano M, Blasco MA. Telomeres acquire embryonic stem cell characteristics in induced pluripotent stem cells. *Cell Stem Cell* 2009;4:141–154. [PubMed: 19200803]
11. Lowry WE, Plath K. The many ways to make an iPS cell. *Nat Biotechnol* 2008;26:1246–1248. [PubMed: 18997764]
12. Aoi T, Yae K, Nakagawa M, Ichisaka T, Okita K, Takahashi K, Chiba T, Yamanaka S. Generation of pluripotent stem cells from adult mouse liver and stomach cells. *Science* 2008;321:699–702. [PubMed: 18276851]
13. Ebert AD, Yu J, Rose FF Jr, Mattis VB, Lorson CL, Thomson JA, Svendsen CN. Induced pluripotent stem cells from a spinal muscular atrophy patient. *Nature* 2009;457:277–280. [PubMed: 19098894]
14. Dimos JT, Rodolfa KT, Niakan KK, Weisenthal LM, Mitsumoto H, Chung W, Croft GF, Saphier G, Leibel R, Golland R, Wichterle H, Henderson CE, Eggan K. Induced pluripotent stem cells generated from patients with ALS can be differentiated into motor neurons. *Science* 2008;321:1218–1221. [PubMed: 18669821]
15. Hanna J, Wernig M, Markoulaki S, Sun CW, Meissner A, Cassady JP, Beard C, Brambrink T, Wu LC, Townes TM, Jaenisch R. Treatment of sickle cell anemia mouse model with iPS cells generated from autologous skin. *Science* 2007;318:1920–1923. [PubMed: 18063756]
16. Wernig M, Zhao JP, Pruszak J, Hedlund E, Fu D, Soldner F, Broccoli V, Constantine-Paton M, Isacson O, Jaenisch R. Neurons derived from reprogrammed fibroblasts functionally integrate into the fetal

- brain and improve symptoms of rats with Parkinson's disease. *Proc Natl Acad Sci USA* 2008;105:5856–5861. [PubMed: 18391196]
17. Xu D, Alipio Z, Fink LM, Adcock DM, Yang J, Ward DC, Ma Y. Phenotypic correction of murine hemophilia A using an iPS cell-based therapy. *Proc Natl Acad Sci USA* 2009;106:808–813. [PubMed: 19139414]
 18. Schenke-Layland K, Rhodes KE, Angelis E, Butylkova Y, Heydarkhan-Hagvall S, Gekas C, Zhang R, Goldhaber JI, Mikkola HK, Plath K, MacLellan WR. Reprogrammed mouse fibroblasts differentiate into cells of the cardiovascular and hematopoietic lineages. *Stem Cells* 2008;26:1537–1546. [PubMed: 18450826]
 19. Narazaki G, Uosaki H, Teranishi M, Okita K, Kim B, Matsuoka S, Yamanaka S, Yamashita JK. Directed and systematic differentiation of cardiovascular cells from mouse induced pluripotent stem cells. *Circulation* 2008;118:498–506. [PubMed: 18625891]
 20. Mauritz C, Schwanke K, Reppel M, Neef S, Katsirntaki K, Maier LS, Nguemo F, Menke S, Hausteiner M, Hescheler J, Hasenfuss G, Martin U. Generation of functional murine cardiac myocytes from induced pluripotent stem cells. *Circulation* 2008;118:507–517. [PubMed: 18625890]
 21. Zhang J, Wilson GF, Soerens AG, Koonce CH, Yu J, Palecek SP, Thomson JA, Kamp TJ. Functional cardiomyocytes derived from human induced pluripotent stem cells. *Circ Res* 2009;104:e30–e41. [PubMed: 19213953]
 22. Nelson TJ, Martinez-Fernandez A, Yamada S, Mael AA, Terzic A, Ikeda Y. Promiscuous human stemness related factors induce interspecies pluripotent reprogramming. *Clin Translation Sci* 2009;2:118–126.
 23. Hasegawa K, Nakamura T, Harvey M, Ikeda Y, Oberg A, Figini M, Canevari S, Hartmann LC, Peng KW. The use of a tropism-modified measles virus in folate receptor–targeted virotherapy of ovarian cancer. *Clin Cancer Res* 2006;15:6170–6178. [PubMed: 17062694]
 24. Perez-Terzic C, Faustino RS, Boorsma BJ, Arrell DK, Niederländer NJ, Behfar A, Terzic A. Stem cells transform into a cardiac phenotype with remodeling of the nuclear transport machinery. *Nat Clin Pract Cardiovasc Med* 2007;4:S68–S76. [PubMed: 17230218]
 25. Yamada S, Nelson TJ, Crespo-Diaz RJ, Perez-Terzic C, Liu XK, Miki T, Seino S, Behfar A, Terzic A. Embryonic stem cell therapy of heart failure in genetic cardiomyopathy. *Stem Cells* 2008;26:2644–2653. [PubMed: 18669912]
 26. Behfar A, Perez-Terzic C, Faustino RS, Arrell DK, Hodgson DM, Yamada S, Puceat M, Niederländer N, Alekseev AE, Zingman LV, Terzic A. Cardiopoietic programming of embryonic stem cells for tumor-free heart repair. *J Exp Med* 2007;204:405–420. [PubMed: 17283208]
 27. Behfar A, Zingman LV, Hodgson DM, Rauzier JM, Kane GC, Terzic A, Puceat M. Stem cell differentiation requires a paracrine pathway in the heart. *FASEB J* 2002;16:1558–1566. [PubMed: 12374778]
 28. Nelson TJ, Martinez-Fernandez A, Terzic A. *KCNJ11* knockout morula reengineered by stem cell diploid aggregation. *Phil Trans R Soc B* 2009;364:269–276. [PubMed: 18977736]
 29. Nelson TJ, Faustino RS, Chiriack A, Crespo-Diaz R, Behfar A, Terzic A. CXCR4⁺/FLK-1⁺ biomarkers select a cardiopoietic lineage from embryonic stem cells. *Stem Cells* 2008;26:1464–1474. [PubMed: 18369102]
 30. Nelson TJ, Chiriack A, Faustino RS, Crespo-Diaz RJ, Behfar A, Terzic A. Lineage specification of Flk-1⁺ progenitors is associated with divergent Sox7 expression in cardiopoiesis. *Differentiation* 2009;77:248–255. [PubMed: 19272523]
 31. Park IH, Arora N, Huo H, Maherali N, Ahfeldt T, Shimamura A, Lensch MW, Cowan C, Hochedlinger K, Daley GQ. Disease-specific induced pluripotent stem cells. *Cell* 2008;134:877–886. [PubMed: 18691744]
 32. Kim JB, Zaehres H, Wu G, Gentile L, Ko K, Sebastiano V, Araúzo-Bravo MJ, Ruau D, Han DW, Zenke M, Schöler HR. Pluripotent stem cells induced from adult neural stem cells by reprogramming with two factors. *Nature* 2008;454:646–650. [PubMed: 18594515]
 33. Yamanaka S. Pluripotency and nuclear reprogramming. *Philos Trans R Soc Lond B Biol Sci* 2008;363:2079–2087. [PubMed: 18375377]
 34. Nelson TJ, Behfar A, Terzic A. Strategies for therapeutic repair: The “R3” regenerative medicine paradigm. *Clin Translation Sci* 2008;1:168–171.

35. Yang X, Smith SL, Tian XC, Lewin HA, Renard JP, Wakayama T. Nuclear reprogramming of cloned embryos and its implications for therapeutic cloning. *Nat Genet* 2007;39:295–302. [PubMed: 17325680]
36. Okita K, Nakagawa M, Hyenjong H, Ichisaka T, Yamanaka S. Generation of mouse induced pluripotent stem cells without viral vectors. *Science* 2008;322:949–953. [PubMed: 18845712]
37. Stadtfeld M, Nagaya M, Utikal J, Weir G, Hochedlinger K. Induced pluripotent stem cells generated without viral integration. *Science* 2008;322:945–949. [PubMed: 18818365]
38. Woltjen K, Michael IP, Mohseni P, Desai R, Mileikovsky M, Hämäläinen R, Cowling R, Wang W, Liu P, Gertsenstein M, Kaji K, Sung HK, Nagy A. piggyBac transposition reprograms fibroblasts to induced pluripotent stem cells. *Nature* 2009;458:766–770. [PubMed: 19252478]
39. Anversa P, Leri A, Rota M, Hosoda T, Bearzi C, Urbanek K, Kajstura J, Bolli R. Stem cells, myocardial regeneration, and methodological artifacts. *Stem Cells* 2007;25:589–601. [PubMed: 17124006]
40. Gnecci M, Zhang Z, Ni A, Dzau VJ. Paracrine mechanisms in adult stem cell signaling and therapy. *Circ Res* 2008;103:1204–1219. [PubMed: 19028920]
41. Wu SM, Chien KR, Mummery C. Origins and fates of cardiovascular progenitor cells. *Cell* 2008;132:537–543. [PubMed: 18295570]
42. Chien KR, Domian IJ, Parker KK. Cardiogenesis and the complex biology of regenerative cardiovascular medicine. *Science* 2008;322:1494–1497. [PubMed: 19056974]
43. Singla DK, Hacker TA, Ma L, Douglas PS, Sullivan R, Lyons GE, Kamp TJ. Transplantation of embryonic stem cells into the infarcted mouse heart: formation of multiple cell types. *J Mol Cell Cardiol* 2006;40:195–200. [PubMed: 16288779]
44. Hodgson DM, Behfar A, Zingman LV, Kane GC, Perez-Terzic C, Alekseev AE, Pucéat M, Terzic A. Stable benefit of embryonic stem cell therapy in myocardial infarction. *Am J Physiol Heart Circ Physiol* 2004;287:H471–479. [PubMed: 15277190]
45. Kolossov E, Bostani T, Roell W, Breitbach M, Pillekamp F, Nygren JM, Sasse P, Rubenchik O, Fries JW, Wenzel D, Geisen C, Xia Y, Lu Z, Duan Y, Kettenhofen R, Jovinge S, Bloch W, Bohlen H, Welz A, Hescheler J, Jacobsen SE, Fleischmann BK. Engraftment of engineered ES cell-derived cardiomyocytes but not BM cells restores contractile function to the infarcted myocardium. *J Exp Med* 2006;203:2315–2327. [PubMed: 16954371]
46. Blomer U, Gruh I, Witschel H, Haverich A, Martin U. Shuttle of lentiviral vectors via transplanted cells in vivo. *Gene Therapy* 2005;12:67–74. [PubMed: 15385952]
47. Strang BL, Takeuchi Y, Relander T, Richter J, Bailey R, Sanders DA, Collins MK, Ikeda Y. Human immunodeficiency virus type 1 vectors with alphavirus envelope glycoproteins produced from stable packaging cells. *J Virol* 2005;79:1765–1771. [PubMed: 15650201]
48. Passier R, van Laake LW, Mummery CL. Stem-cell-based therapy and lessons from the heart. *Nature* 2008;453:322–329. [PubMed: 18480813]
49. Nelson TJ, Behfar A, Terzic A. Stem cells: biologics for regeneration. *Clin Pharmacol Ther* 2008;84:620–623. [PubMed: 18701884]
50. Roell W, Lewalter T, Sasse P, Tallini YN, Choi BR, Breitbach M, Doran R, Becher UM, Hwang SM, Bostani T, von Maltzahn J, Hofmann A, Reining S, Eiberger B, Gabris B, Pfeifer A, Welz A, Willecke K, Salama G, Schrickel JW, Kotlikoff MI, Fleischmann BK. Engraftment of connexin 43-expressing cells prevents post-infarct arrhythmia. *Nature* 2007;450:819–824. [PubMed: 18064002]

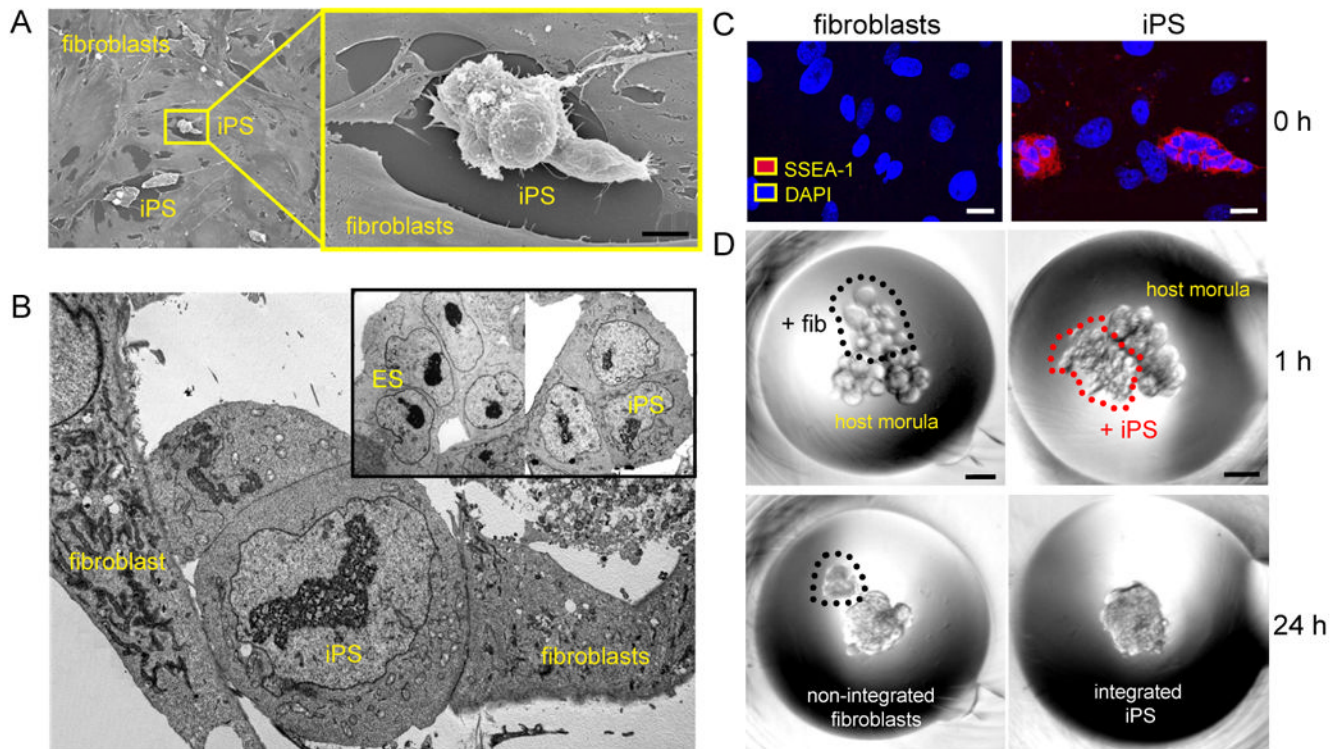


Figure 1.

Induced pluripotent stem cells (iPS) demonstrate pluripotent features. A, Flat fibroblasts reprogrammed with human stemness factors metamorphosed into rounded clusters shown by field-emission scanning electron microscopy. Bar=50 μm . B, In transmission electron microscopy, derived iPS demonstrated nuclear/cytoplasmic composition similar to embryonic stem cells (ES). C, Counterstained by nuclear DAPI, iPS expressed the pluripotent marker SSEA-1 (red), absent from fibroblasts (0 h; left). Bar=5 μm . D, Fibroblasts or iPS clumps were placed along with two 8-cell host embryos for diploid aggregation (1 h; top). Bar=30 μm . Within 24 h, iPS spontaneously integrated to form an early stage chimeric blastocyst (24 h; bottom right), in contrast to fibroblasts that were excluded (24 h; bottom left).

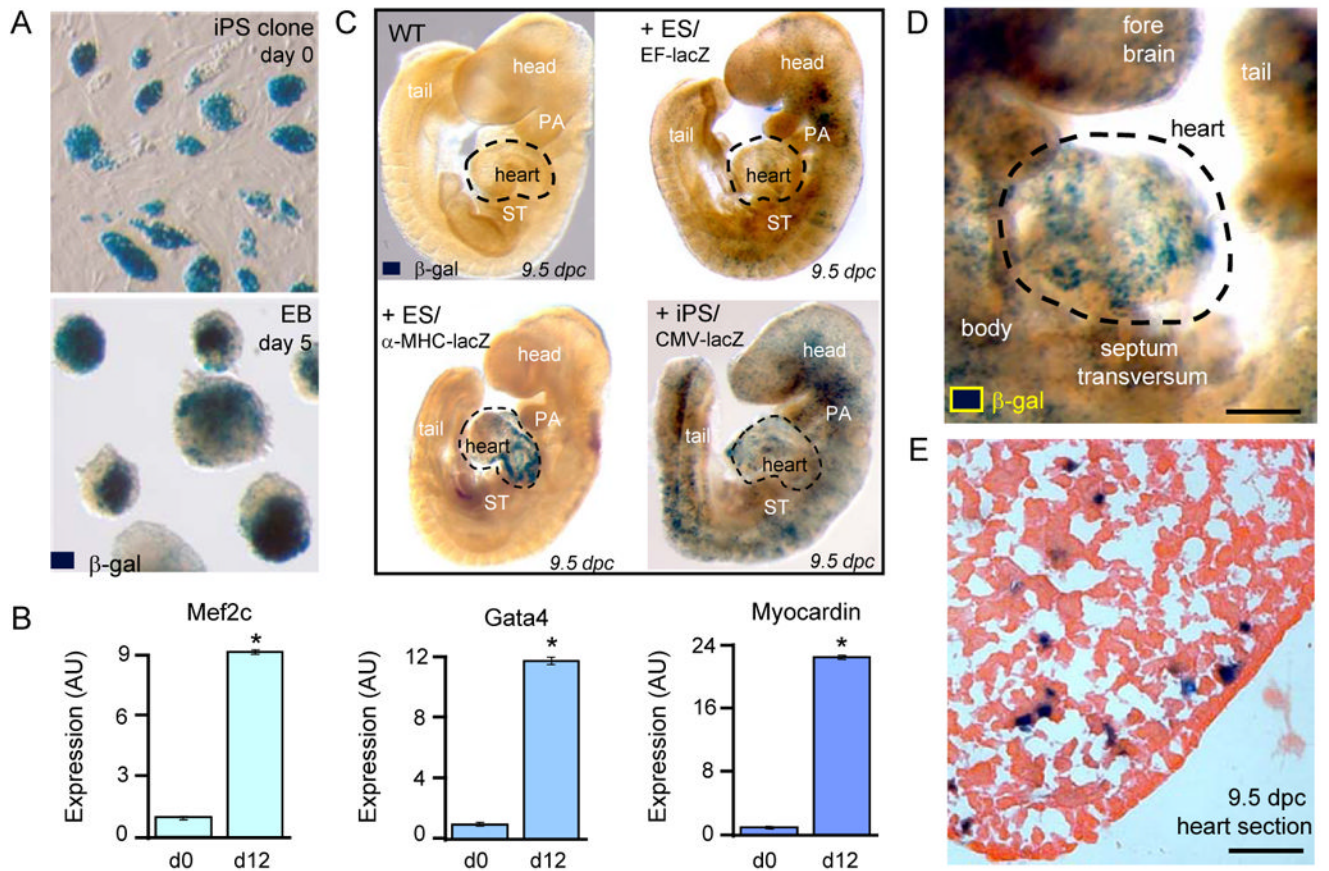


Figure 2.

iPS recapitulate *in utero* cardiogenic propensity. A, LacZ-labeled iPS clones, detected by β-galactosidase (β-gal) staining, were maintained as undifferentiated colonies at day 0 before aggregation into embryoid bodies (EB). B, Gene expression profiles at day 0 (d0) compared to day 12 (d12) of differentiation demonstrated induction of cardiac transcription factors, Mef2c (p=0.049; n=3), Gata4 (p=0.049; n=3), and Myocardin (p=0.049; n=3). C, Embryos provide a wildtype (WT) environment to determine tissue-specific differentiation (upper left). Derived by diploid aggregations, ES stochastically contribute to tissue patterning with diffuse integration tracked with constitutively labelled EF-lacZ cell line (upper right) and cardiac-specific integration identified by α-MHC-lacZ reporter (lower left). iPS, labeled with ubiquitously expressing reporter with CMV promoter, identifies progeny throughout developing embryo (lower right). D, Chimerism with lacZ-labeled iPS demonstrated robust contribution to developing hearts within 9.5 dpc embryos. Bar=100 μm. E, Heart parenchyma of 9.5 dpc chimeric embryo contained integrated iPS progeny expressing β-galactosidase. Bar=50 μm.

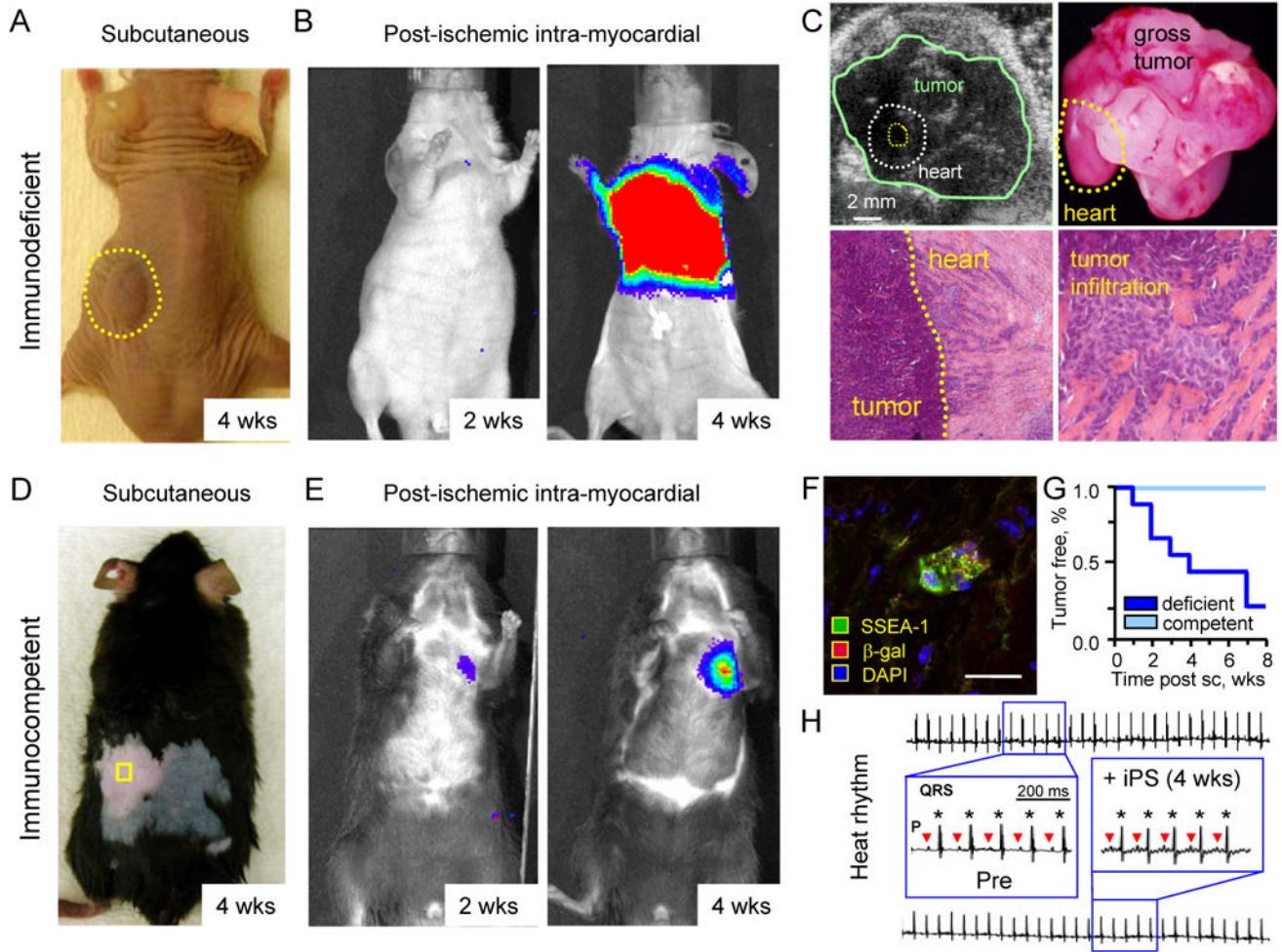


Figure 3. iPS fate determined by host competency. A, Subcutaneous injection of 500,000 iPS in immunodeficient host resulted in tumor growth (dotted circle). B, Upon acute myocardial infarction, 200,000 iPS transplanted intra-myocardially were detected in the heart region by *in vivo* bioluminescence imaging dramatically expanding by 4 weeks (wks). C, Tumor growth was detected by echocardiography (upper left) and confirmed on necropsy in all immunodeficient hosts (upper right). Histology demonstrated tumor expansion outside of the heart (lower left), and infiltration within the wall of infarcted myocardium (lower right). D, Immunocompetent hosts reproducibly averted tumor growth upon subcutaneous injection (square) of 500,000 iPS throughout follow-up. E, iPS transplantation within infarcted myocardium of immunocompetent hosts produced stable engraftment detected by live-cell imaging throughout the 4 week follow-up. F, Post-ischemic myocardium transplanted with iPS at 4 weeks demonstrated rare pockets of SSEA-1 positive progeny. Bar=10 μ m. G, Subcutaneous (sc) transplantation produced teratoma in immunodeficient (deficient), in contrast to tumor-free outcome in all immunocompetent (competent) hosts. H, Normal pre-infarction (Pre) sinus rhythm was maintained following iPS transplantation throughout the 4 week follow-up, with P-waves (triangles) preceding each QRS complex (stars) with no ventricular tachycardia or ectopy.

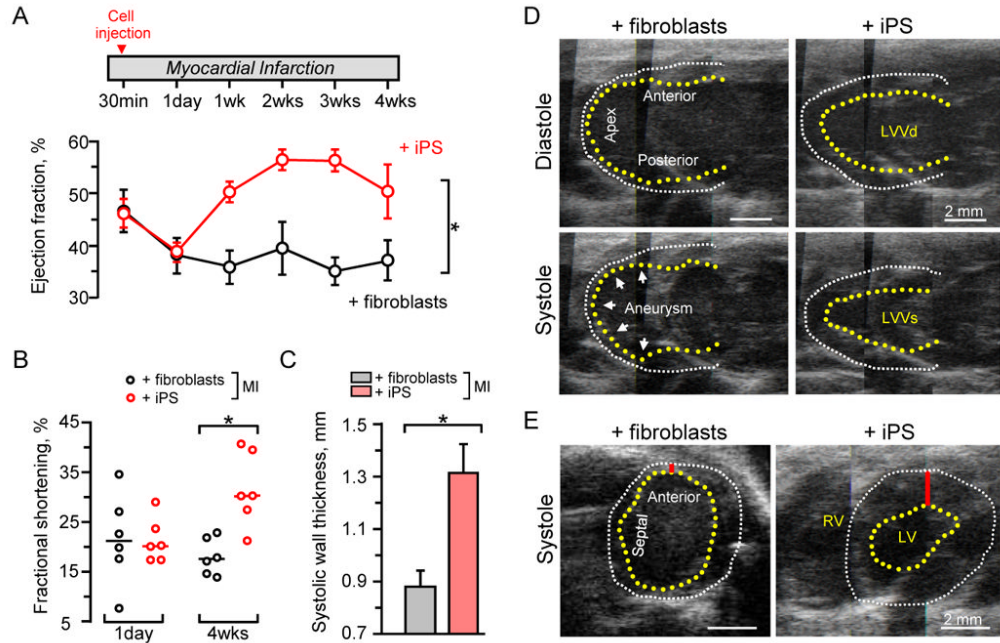


Figure 4.

iPS restored function following acute myocardial infarction (MI). A, Upon randomization, cell-based intervention was performed at 30 min after coronary ligation. Divergent ejection fractions were noted in iPS (n=6) versus fibroblast (n=6) treated hearts within 1 week post-therapy, maintained throughout follow-up. *p=0.002 using two-way repeated measures ANOVA. B, Fractional shortening was similar at day 1 post-infarction, but significant improvement was only observed in iPS-treated hearts. Line indicates median value. *p=0.01. C, Septal wall thickness was preserved in systole following iPS (n=6) compared to fibroblast (n=6) treatment. *p=0.006. D, Echocardiography with long-axis views revealed anterior wall thinning and apex aneurysmal formation (arrow heads) in fibroblast-treated hearts as indicated by akinetic wall (left) in contrast to normalized systolic wall motion in iPS-treated hearts (right). E, Short-axis confirmed thinning in the anterior wall (red bar) and overall decreased cardiac performance with fibroblast compared to iPS-based interventions. Yellow and white dotted lines indicate endocardium and epicardium, respectively. LVVd: left ventricular volume in diastole; LVVs: left ventricular volume in systole.

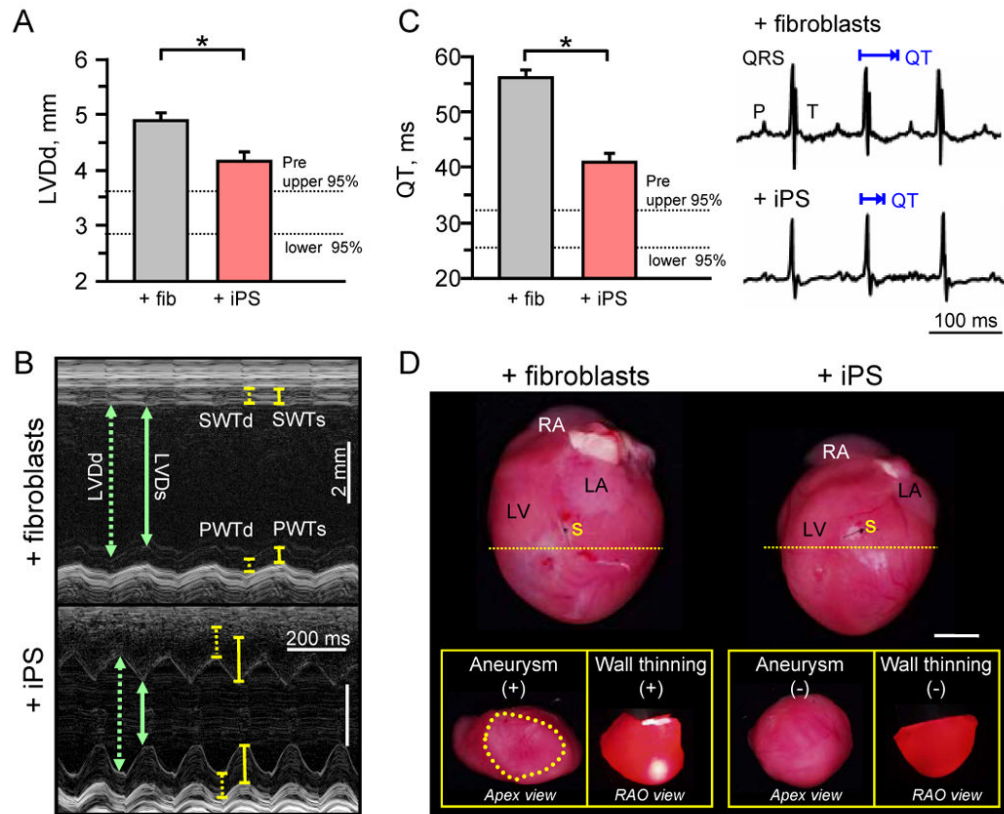


Figure 5.

iPS halt maladaptive remodeling and preserve structure. A, Diastolic parameters revealed a significant decrease in global left ventricular diastolic diameter (LVDD) in hearts treated with iPS (n=6) compared to fibroblasts (n=6) at 4-weeks post-therapy (*p=0.007). B, M-mode echocardiography demonstrated dilated ventricular lumen with reduced anterior and septal wall thickness (SWTd) during systole in fibroblast-treated hearts (upper), which improved with iPS intervention (lower). C, Time required for ventricular repolarization and depolarization, measured by the QT interval, was significantly prolonged in fibroblast (n=6) compared to iPS (n=6) treated hearts. *p=0.004. D, Hearts were pathologically enlarged in the fibroblast-treated group with aneurysmal formation (+) and severe wall thinning (+) visible with transillumination compared to structurally preserved iPS-treated hearts with normal apex geometry (-) and opaque thick walls (-) on right anterior-oblique (RAO) view upon transverse sectioning of hearts immediately inferior to the site of surgical ligation (yellow dotted line). Bar=5mm. Aneurysm delineated by yellow dotted circle. RA: right atrium; LA: left atrium; LV: left ventricle; s: suture; SWTd: septal wall thickness in diastole; SWTs: septal wall thickness in systole; PWTd: posterior wall thickness in diastole; PWTs: posterior wall thickness in systole.

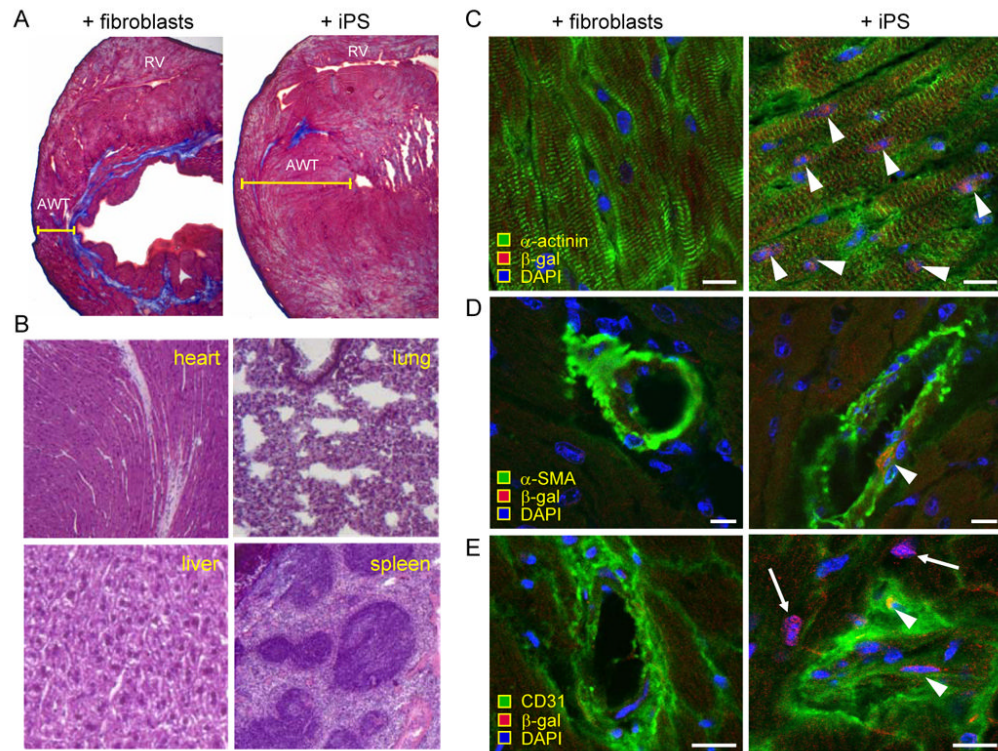


Figure 6. iPS treatment reduced scar and contributed to multi-lineage reconstruction. A, After 4 week of therapy, Masson's trichrome staining demonstrated reduced anterior wall thickness (AWT) and fibrosis (blue staining) in hearts treated with fibroblasts (left) compared to iPS (right). B, Autopsy demonstrated tumor-free heart, liver, lung, or spleen in the iPS-treated cohort. C, After 4 weeks, integrated iPS progeny expressed markers of remuscularization according to α -actinin (right) and β -gal co-expression (arrow heads), not detectable with fibroblast treatment (left). D, Smooth muscle actin (α -SMA; arrow head), and E, CD31 positive endothelium (arrow heads) were identified in iPS progeny (right) compared to no expression with fibroblast treatment (left). DAPI visualized nuclei. Bar=5 μ m.